A framework for predicting the dynamics of plant-mycorrhizal interactions

Tanner Dulay[1,2], Angelica Soriano[1], Priyanga Amarasekare[1]

[1] Dept. of Ecology and Evolutionary Biology, University of California, Los Angeles
[2] Corresponding author: tdulay@g.ucla.edu

Short title: Plant-Mycorrhizal Interactions Model

Word Count (Main text): 5452 (Abstract: 180)

Manuscript Content: Abstract, Introduction, Mathematical Framework, Model Analysis, Results, Discussion, 2 Tables, 4 Figures, Literature Cited, 1 Appendix

Abstract

Interactions between plants and mycorrhizal fungi shape nutrient cycling and ecosystem function on a global scale, but the dynamics of these interactions remain poorly understood. Due to their below-ground nature, directly observing key dynamical features such as Allee effects and oscillations is often not possible, hampering further progress in this area. Here we present a mechanistic model of plant-mycorrhizal interactions to address this issue. By integrating the facilitative and the antagonistic elements of plant-mycorrhizal interactions with explicit plant-nutrient dynamics, our framework generates testable predictions about the dynamics and persistence of these interactions. We find that plant-mycorrhizal interactions can exhibit different dynamical realms ranging from Allee effects to consumer-resource oscillations, and that these dynamics can be inferred from measurable system parameters (e.g., nutrient or carbohydrate uptake rates and saturation constants) and plant/fungal biomasses. Furthermore, we find that changes in the underlying soil nutrient supply can induce changes from one dynamical realm to another. Finally, we present a decision tree framework for characterizing the dynamics of real systems and discuss implications of our findings for plant-mycorrhizal communities in applied and natural contexts.

Keywords: mycorrhizae, mutualism, species interactions, mechanistic model, nutrient limitation

Introduction

Interactions between plants and mycorrhizal fungi are ubiquitous, occurring in ca. 80% of plant species and contributing substantially to global nutrient cycling and ecosystem services (Brundrett, 2009; van der Heijden et al., 2015; Wang & Qiu, 2006). Whether fungal hyphae

penetrate plant roots as in arbuscular mycorrhizae (AMF) or form a sheath around the roots as in ectomycorrhizae (ECM), mycorrhizal fungi facilitate plant acquisition of soil nutrients such as Nitrogen, Phosphorous, and water (Smith & Read, 2010). In return, plant hosts provide their fungal partners with a source of carbohydrates (Fellbaum et al., 2012). These interactions play a foundational role in supporting terrestrial biodiversity and have been widely proposed as sustainable tools to increase crop yield and facilitate restoration efforts (Asmelash et al., 2016; Fester & Sawers, 2011; Neuenkamp et al., 2019; Solaiman & Mickan, 2014). However, owing to their strong context-dependence and below-ground nature impeding comprehensive empirical studies, we currently lack the understanding of plant-mycorrhizal dynamics necessary to consistently predict their functioning in applied and natural contexts.

Despite their promise of enhancing agriculture and restoration, the application of mycorrhizal fungi in these settings often yields inconsistent results. Although commercially available fungal inoculants can decrease the need for fertilizers in agricultural soils, their effect on crop yield can range from substantial increases to neutral or even negative impacts depending on soil conditions, plant host identity, and existing microbial communities (Hart & Reader, 2002; Hoeksema et al., 2010; Koziol et al., 2024; Ryan & Graham, 2002). In restoration, mycorrhizae are suggested to facilitate the reintroduction of native plant species and support community resilience (Asmelash et al., 2016; Solaiman & Mickan, 2014). In practice, however, it can be hard to predict whether an introduced fungal strain will establish, persist, or interact beneficially with target plant species (Maltz & Treseder, 2015; Neuenkamp et al., 2019; Verbruggen et al., 2013). Our ability to predict outcomes in natural systems is similarly hampered. Although multiple anthropogenic impacts are expected to degrade mycorrhizal diversity (Steidinger et al., 2020; Van Diepen et al., 2007; Vogelsang & Bever, 2009), we do not fully understand how

46 species losses, replacements, or functional shifts caused by environmental perturbations will
47 affect the function and stability of the ecosystems in which they are embedded (Sapsford et al.,
48 2017; Staddon et al., 2002). All of these challenges stem from an incomplete understanding of
49 the dynamics of plant-mycorrhizal interactions.

50 Given the complex interplay of facilitation and consumption, plant-mycorrhizal
51 interactions likely exhibit a diverse array of dynamics. As mutualisms in which at least one
52 partner is typically obligate (as the fungus is in most AMF and ECM; Smith & Read, 2010),
53 plant-mycorrhizal interactions are thought to be subject to Allee effects – thresholds of
54 abundance below which the interaction goes deterministically extinct (Hale & Valdovinos, 2021;
55 Stephens et al., 1999). When assembling interactions from the ground up, as in agricultural and
56 restoration contexts, Allee effects may prevent the establishment of plants or fungi introduced at
57 an insufficient biomass (Armstrong & Wittmer, 2011). On the other hand, because plant-
58 mycorrhizal interactions include a consumer-resource element (Holland & DeAngelis, 2010),
59 they could exhibit oscillations in abundance that may also cause inoculations to fail due to
60 extinction at low abundances. Indeed, a previous model by Neuhauser and Fargione (2004)
61 suggests that plant-mycorrhizal interactions should exhibit both Allee effects and consumer-
62 resource oscillations. This model, however, did not include nutrient-plant dynamics, the key
63 element that connect below-ground and above-ground processes. This makes it difficult to
64 ascertain whether a combination of Allee effects and oscillations drives the dynamics of real
65 plant-mycorrhizal systems.

66 We are not aware of any studies that have directly observed the dynamics of plant-
67 mycorrhizal communities. This is most likely due to the below-ground nature of these
68 interactions precluding the repeated fine-scale observations necessary to identifying dynamics.

Further complicating the matter is the finding that the dynamics of plant-mycorrhizal interactions are strongly context-dependent, varying by nutrient availability, light intensity, host plant identity, and other factors (Bryant & Bever, n.d.; Hoeksema et al., 2010; Koorem et al., 2017). Addressing these challenges requires a theoretical framework that incorporates this context dependence in generating predictions about dynamics and long-term persistence of plant-mycorrhizal interactions. Although existing theory has improved our understanding of plant-mycorrhizal interactions, the models used are largely phenomenological models and cannot make predictions that can guide specific empirical systems (Hale & Valdovinos, 2021; Neuhauser & Fargione, 2004). We need mechanistic theory that is rooted in the biology of plant-mycorrhizal interactions that can predict outcomes in terms of measurable parameters and state variables.

Here we take a first step toward addressing this key gap in our knowledge. We develop a mechanistic model of plant-mycorrhizal interactions that integrates the facilitative and consumptive aspects of the interaction with explicit nutrient-plant dynamics. By parameterizing the model with empirical data from the literature, we generate predictions about the range of dynamical outcomes that are likely to occur in real plant-mycorrhizal systems. We specifically explore the context-dependence of plant-mycorrhizal dynamics along a gradient of nutrient availability. We frame our findings in terms of measurable parameters (e.g., soil nutrient supply) and variables (e.g., biomass) that researchers working in plant-mycorrhizal systems can use to identify dynamical patterns in the real communities.

Mathematical Framework

We consider a closed system with a constant nutrient input in which the total nutrient availability sets the upper limit to the total biomass. This is a reasonable assumption given biological stoichiometric constraints and mechanisms maintaining nutrient limitation in

terrestrial ecosystems (Ågren et al., 2012; Menge et al., 2009; Vitousek et al., 1998). The plant species' growth and reproduction depend on an essential nutrient (e.g., Nitrogen, Phosphorous), for which the individuals in the plant population compete. The nutrient is returned to the soil in turn through plant turnover and metabolic losses (i.e., leaf litter, root turnover, plant mortality). The plant may form an association with a mycorrhizal fungus that facilitates nutrient uptake in exchange for carbohydrates that the plant produces via photosynthesis. We consider the *de novo* assembly of the plant-mycorrhizal interaction in an initially empty habitat.

Initial colonizers of empty habitats (e.g., early successional plant species) tend to exhibit strategies for resource acquisition that do not depend on mutualistic partners (Nara, 2006b; Tilman, 1986). Initial colonizers are likely to be plant species that can acquire nutrients in the absence of mycorrhizal fungi but have a higher nutrient uptake rate in the presence of such fungi (Nara, 2006a). Secondary colonizers can be either facultative or obligate in their reliance on mutualists for nutrient acquisition. Most mycorrhizal fungi are obligate root symbionts and therefore dependent on the plant for carbon (Smith & Read 2010). We therefore consider situations in which the plant can be either obligate or facultative on the benefits conferred by mycorrhizal fungi, while the fungus always requires a plant host in order to grow. Both spores and dormant hyphae in the soil are sources by which fungi encounter and form mycorrhizae with plant roots (McGEE et al., 1997; Pepe et al., 2018; Schubert et al., 1987).

Mycorrhizal fungi that associate with plant roots constitute two major types. Arbuscular mycorrhizal fungi (AMF) enter the host plant's root system, while ectomycorrhizal fungi (ECM) form a hyphal sheath around the plant's roots without penetrating them. In both cases, the fungal hyphae extend from roots into the surrounding soil to forage for nutrients (predominantly Phosphorous in the case of AMF, both Nitrogen and Phosphorous in varying degrees in the case

of ECM; van der Heijden et al., 2015), which are then transferred to the plant in exchange for photosynthates across the root-hyphae interface (Fellbaum et al., 2012). When the benefit of nutrient uptake exceeds biomass consumption, the fungus acts as a facilitator; when biomass consumption exceeds the benefit provided to the plant, the fungus acts as an antagonist (a consumer rather than a facilitator).

We formalize these ideas in the following mathematical model:

$$\frac{dN(t)}{dt} = b\big(S - N(t)\big) - a_P e_P P(t) N(t)\left(\frac{A(t)}{A(t)+M} + r_P\right) + e_P d_P P(t) + e_A d_A A(t)$$

$$\frac{dP(t)}{dt} = a_P\left(\frac{A(t)}{A(t)+M} + r_P\right) N(t) P(t) - m_{AP}\left(\frac{P(t)}{P(t)+H}\right) A(t) - d_P P(t) \qquad (1)$$

$$\frac{dA(t)}{dt} = \frac{e_P}{e_A} m_{AP}\left(\frac{P(t)}{P(t)+H}\right) A(t) - d_A A(t)$$

Where S is the soil nutrient supply point, b is the nutrient turnover rate, $N(t)$ is the nutrient availability at time t, and $P(t)$ and $A(t)$ denote, respectively, the biomasses of the plant and mycorrhizal fungus. The parameters e_P and e_A depict the nutrient to Carbon ratios, i.e., the number of grams of nutrient contained in one gram of plant and fungal biomass, respectively. Both facilitation of nutrient uptake by plants and plant biomass consumption by the fungus are given by Monod functions (Monod, 1949). The plant's nutrient acquisition rate is a saturating function of fungal density where a_P is the maximum nutrient uptake rate, achieved only in the presence of its mycorrhizal partner, and M is the biomass density of the fungus at which the plant species' uptake rate is half its maximum ($a_P/2$). The parameter r_P is the fractional reduction in the uptake rate in the absence of the fungus, *i.e.*, in the absence of facilitation of nutrient uptake by the fungus, the plant species' nutrient uptake rate is $r_P\, a_P$ ($r_P = 0$ when the plant cannot survive

in the absence of the fungus). Of note, although this formulation means the theoretical maximum nutrient uptake rate the plant can attain is $(1 + r_P) * a_P > a_P$ as $A(t) \to \infty$, in our study fungal biomass is never high enough for the maximum $(1 + r_P) * a_P$ to exceed a_P. We therefore retain this formulation as it provides for greater analytical tractability. The fungal strain's maximum carbohydrate consumption rate is m_{AP} and H is the biomass density of the plant at which the fungus's uptake rate is $m_{AP}/2$. Nutrient is returned to the soil through plant and fungal metabolic losses (e.g., mortality) with rates d_P and d_A, respectively.

When the system is closed (e.g., in the limit that the turnover rate b is on the same order as the mortality rates d), the equation for nutrient dynamics can be replaced with the following mass balance constraint (Grover, 1994; Loreau, 1994, 1995):

$$N(t) = S - e_P P(t) - e_A A(t)$$

Preliminary analyses indicate that the results are qualitatively similar when we use explicit nutrient dynamics (Equation (1)) rather than the mass balance constraint. We conduct all analyses of the model using the mass balance constraint.

Of note, our model formulation is such that nutrient dynamics are explicitly modeled rather than phenomenologically incorporated via a carrying capacity. This allows for a mechanistic exploration of population dynamics and the measurable parameters that drive the dynamics. In addition, our model is not specific to a particular nutrient or type of root-hyphal interface and thus provides a general framework that is applicable to any type of mycorrhizal association (e.g., AMF, ECM, etc).

Phase plane analysis of Equation (1) combined with asymptotic analysis of long-term outcomes (Appendix 1) yields insights into the dynamical behavior of the plant-fungal

154 interaction. Depending on the relative costs and benefits to the plant based on its association with
155 the fungus, the system can exist in three dynamical realms:

156 1. When the benefits to the plant provided by the fungus exceed the costs they incur, the
157 plant's abundance at equilibrium in the presence of the fungus ($P^*|_{A^*>0}$) exceeds that in
158 the absence of the fungus ($P^*|_{A^*=0}$), causing the fungal strain's zero growth isocline to
159 cross closer to the vertex of the plant species' zero growth isocline (Fig. 1(a)). This
160 generates an Allee effect with two interior equilibria, the lower of which is unstable and
161 the higher of which is locally stable (see Appendix 1 for details). As a result, when plant
162 or fungal abundance falls below the lower interior equilibrium, the interaction goes
163 deterministically extinct.
164 2. When the benefit to the plant is less than the cost, $P^*|_{A^*>0} < P^*|_{A^*=0}$ and the fungal isocline
165 crosses further away from the vertex and closer to the y-axis (Fig.1(b)). Now there is
166 only a single interior equilibrium, which can be a stable focus attained via damped
167 oscillations or an unstable focus surrounded by persistent oscillations (Appendix 1).
168 3. When r_P tends to zero, the plant becomes increasingly dependent on the fungus (the plant
169 is obligate when $r_P = 0$), and there is no longer a boundary equilibrium with only the
170 plant species present (Fig. 1(c)).

171 Of note, despite the fact that the fungus provides a benefit to the plant in facilitating nutrient
172 acquisition, their interaction is that between a consumer and resource. This can be shown
173 formally by inspecting the elements of the Jacobian matrix of Equation (1). The off-diagonal
174 elements have opposite signs such that the plant has a positive effect on the fungus while the
175 fungus has a negative effect on the plant (see Appendix 1 for details). This is because the plant
176 species' equilibrium biomass in the presence of the fungus is independent of M, the parameter

that determines the fungus' beneficial effect on the plant. This is one of the few instances we are aware of in which an Allee effect emerges naturally in a mechanistic consumer-resource model.

The dynamical behavior of the plant-fungal interaction depends on six key parameters ($a_P, r_P, M, m_{AP}, H,$ and S). The system exhibits an Allee effect and multiple equilibria when a_P and r_P are low (i.e., the plant is more reliant on the fungus for nutrient acquisition) *and* H is high and m_{AP} is low (i.e., the fungus does not remove a large amount of carbohydrate from the plant) (Fig. 1(a) and (b)). The parameter M determines the shape of the plant species' zero growth isocline and the magnitude of the fungal strain's equilibrial biomass (A*). When M is low, the plant isocline has a higher peak and vertex and higher A* than when M is high (compare Fig.1(a) with (d) and (b) with (e)). As noted above, when r_P is high the plant is facultative and can persist on its own, becoming obligate when $r_P \to 0$ (Fig. 1(c)). When S is high, the plant species' isocline has a higher peak and vertex, and $P^*|_{A^*=0} >> P^*|_{A^*>0}$ making an Allee effect less likely (Fig. 1(f)). When S is low, the peak and vertex both shrink, and $P^*|_{A^*=0} << P^*|_{A^*>0,}$ making an Allee effect more likely provided H is high and m_{AP} is low.

Model Analysis

We used numerical simulations to test whether the predictions made based on the phase plane and asymptotic analyses in the previous section are realized when the model is parameterized using empirically observed values. Given that Nitrogen constitutes the most limiting nutrient for most plant species, we considered *S* to depict the soil mineral Nitrogen content. Based on published data (Ansong Omari et al., 2018; Pastor et al., 1987), *S* varies in the range 0.001-7.0 g m^{-2}, with tropical soils containing less mineralized nitrogen than temperate

199 soils. In our analysis we used an average value of S=1.0 g m^{-2}. The mean Nitrogen: Carbon ratios
200 for plants (e_P) and ectomycorrhizal hyphae (e_A) are 0.027 (Elser et al., 2000, 2010) and 0.069
201 (Zhang & Elser, 2017), respectively. Marx et al. (2019) calculate an average maximum nitrogen
202 uptake rate by plants (a_P) of 0.17 ± 0.2 g day^{-1} (mean ± SD). The contribution of
203 ectomycorrhizae to plant nitrogen acquisition, which we use to estimate r_P, varies from 0-80%
204 (van der Heijden et al., 2015), although there are some types of plant-mycorrhizal interactions in
205 which plants are obligate. Metabolic loss rate for plants (d_P) is 0.01 g day^{-1} from Marx et al.
206 (2019). To the best of our knowledge, metabolic theory has yet to be applied in a comparable
207 way to fungi (but see Aguilar-Trigueros et al., 2017), but it is reported that hyphal turnover is
208 rapid compared to plants (Godbold et al., 2006; Staddon et al., 2003). We therefore used the plant
209 loss rate as a lower bound for the fungal metabolic loss rate (d_A). Using empirically observed
210 ranges of the other parameters we calculated the upper bound above which the interaction
211 becomes inviable to be 0.04 g day^{-1}. Since varying the loss rate within this range leads only to
212 quantitative differences in model outcomes, we set the fungal loss rate at 0.03 g day^{-1}. Hobbie
213 and Hobbie (2006) report mycorrhizal fungi consume between 0.08 and 0.17 day^{-1} of the host
214 plant's primary productivity (m_{AP}), although field estimates sometimes vary more widely
215 (Hobbie, 2006; Smith & Read 2010). We did not find published data on the half-saturation
216 densities for plant nutrient uptake rate facilitation (M) or consumption of plant biomass by fungi
217 (H). We conducted a sensitivity analysis, using empirically observed ranges for other
218 parameters, to identify the values of these two parameters that allowed for a viable plant-
219 mycorrhizal interaction.

220 We varied the six parameters our predictions are based on (a_P, r_P, m_{AP}, M, H and S) and
221 fixed the conversion efficiencies and background loss rates of both species at their empirical

values (Table 1). We varied the uptake parameters within the empirically observed ranges: 0.07-0.27 g day^{-1} for a_P and 0.08-0.17 day^{-1} for m_{AP}, and the saturation parameters within the ranges identified in our sensitivity analysis: 0.1-2.0 g for M and 0.08-36.8 g for H. We used 10 evenly spaced values spanning each of these ranges. We varied r_P from 0 when the plant is obligate to 0.2 (plant can attain 20% of its maximum uptake rate in isolation) in increments of 0.05. We varied S as a 20% decrease/increase of the baseline value (S=1.0 g m^{-2}) to test the predictions about the effects of nutrient scarcity/enrichment on plant-fungal dynamics.

For every unique parameter combination delineated in the previous paragraph (N=150,000), we simulated the *de novo* assembly of the plant-mycorrhizal interaction. We initiated each simulation with the plant biomass set to its fungus-free equilibrium ($P^*|_{A=0}$) and the fungal biomass set to zero. After 20 years (7,900 timesteps) we introduced the fungus at a biomass 50% greater than the Allee threshold if an Allee effect was present, or at 0.1 g if there was no Allee effect. We then let each simulation proceed for another 100 years (36,500 timesteps), setting either species biomass to zero if they fell below an extinction threshold of 10^{-10} g. We calculated the average biomasses of the plant and fungus over the last year of the simulation run. All simulations were conducted in Python version 3.8 using the RK45 method employed by the *solve_ivp* function of the *scipy* library.

We conducted two analyses. We first classified the interactions into the three predicted dynamical realms by comparing the long-term outcomes predicted by the phase plane and asymptotic analyses (Fig 1; Appendix 1) with those emerging from the numerical simulations. Cases in which the analytical methods predicted no interior equilibria and simulations showed no positive long-term biomasses for plant or fungus were classified as infeasible. Of the feasible cases, those in which both the plant and fungus had long-term biomasses exceeding the

extinction threshold were classified as persistent interactions. Cases in which the plant species was obligate was identified on the basis of a negative boundary equilibrium (i.e., $Sa_P r_P \leq d_P$; see Appendix 1), and those with an Allee effect on the basis of a positive lower interior equilibrium. Persistent oscillatory interactions were identified based on two criteria: (i) long-term biomasses did not converge to the analytically predicted interior equilibrium, and (ii) the eigenvalues of the Jacobian matrix evaluated at the interior equilibrium had positive real parts.

Our second analysis involved three steps. First, we explored how the parameters a_P, r_P, m_{AP}, M, and H influenced the frequency of the three dynamical realms at the baseline nutrient availability (S=1.0). Second, we varied S by 20% to investigate how nutrient depletion and enrichment influenced plant-mycorrhizal dynamics and long-term dynamics. Third, we used our data to generate decision trees (using *sklearn.tree* and *dtreeviz* packages) – procedural algorithms for diagnosing the likely dynamics of a given system based on the measured values of key parameters. We provide examples of these decision trees for classifying system dynamics based on both the individual parameters as well as combinations of parameters which may be more easily estimated by for real plant-mycorrhizal systems by empiricists.

Results

Identifying dynamical realms

Across the parameter space investigated, 46% of parameter combinations yielded feasible plant-mycorrhizal interactions, half of which constituted persistent plant-fungal interactions in our simulations (22% of all combinations). Of the feasible interactions that did not persist in the long-term, the majority were those in which the plant was obligate and went extinct before the

fungus was introduced (Table 2). The next most frequent case was divergent oscillations leading to deterministic collapse, followed by deterministic extinction via the Allee effect. In the latter case, the initial fungal biomass we introduced, although 50% greater than the Allee threshold, was not sufficiently above the threshold to avoid extinction.

The most frequent dynamical realm observed in our simulations was stable coexistence of the plant and fungus with neither Allee effects nor oscillations (55.2% of persistent interactions; Table 2). The next most frequent were stable (e.g., non-oscillatory) interactions subject to an Allee threshold (28.8%), followed by interactions with persistent oscillations and no Allee effects (15.9%). Interactions exhibiting both persistent oscillations and Allee effects were relatively infrequent (0.1%).

Overall, the distribution of the dynamical realms in our numerical analysis agreed with the analytical predictions made by the phase plane and asymptotic analyses (Figure 1; Appendix 1). As expected, Allee effects (and in more extreme cases, mutually obligate interactions) were more likely when a_P and/or r_P were low, while oscillations (both persistent and divergent) were more likely when H was low and m_{AP} was high (Figure 2). The dynamics of persistent interactions with median-to-high values of a_P and r_P spanned all three realms and were driven largely by H and m_{AP} (lower m_{AP} and higher H led to Allee effects while the reverse led to oscillations; intermediate values produced systems with stable coexistence; Figure 2 (e, f, h)). Infeasible interactions occurred mainly when the fungus was too inefficient a consumer of plant biomass to support itself (Figure 2).

Changes in nutrient supply

Decreasing the nutrient supply point (S) drove more qualitative changes in system dynamics than increasing it. Consistent with our expectations, of the persistent interactions that had no Allee effects at the baseline nutrient supply (S=1.0), 39% exhibited Allee effects under a 20% nutrient reduction (Figure 3). Interactions that exhibited Allee effects at the baseline nutrient supply were prone to collapse under a 20% nutrient reduction, with 75% becoming infeasible due to insufficient nutrient availability to support a viable interaction. Of the persistent interactions that exhibited oscillations under the baseline nutrient supply, 58% remained unchanged while 14% became non-oscillatory, attaining a stable equilibrium, 10% had the plant species become obligate, and 6% became non-oscillatory but exhibited an Allee effect (Figure 3).

Increasing the nutrient supply point by 20% had a less pronounced impact on system dynamics, and changes conformed to our expectations. Most persistent interactions had the same qualitative dynamics following nutrient enrichment, with the exception of 7% of stable interactions becoming oscillatory and Allee effects disappearing from 73% of the interactions that had previously exhibited them (73%). Virtually all oscillatory interactions remained oscillatory following nutrient enrichment.

Decision trees for diagnosing system dynamics

Reflecting the parameter space investigation, our decision tree analysis identified H and m_{AP} as the most instructive in diagnosing dynamics of plant-mycorrhizal interactions. In particular, nearly all oscillatory systems occur when $H < 6.2$ and $m_{AP} > 0.115$ (Figure 4 (a)). However, discerning Allee effects was less effective using the original parameters at the decision tree depth that we used, likely due to the complex nature of the plant-fungal interdependence. We found certain parameter combinations to be more effective at characterizing dynamics: the

plant's nutrient uptake rate in isolation ($a_P * r_P$) and the fungus' consumption efficiency at low plant biomass ($\log[\frac{m_{AP}}{H}]$; Figure 4(b)).

A decision tree trained on the composite parameters was more effective at distinguishing between interactions exhibiting different types of dynamics than the one trained on the original parameters (compare Figures 4(a) and (b)). Persistent oscillations were likely in interactions with high consumption efficiency ($\log\left[\frac{m_{AP}}{H}\right] > -3.598$), save for a small portion of these interactions which also had a high rate of nutrient uptake ($a_P * r_P > 0.0357$) that were more likely to be stable. Allee effects were most likely in systems with low consumption efficiency ($\log\left[\frac{m_{AP}}{H}\right] \leq -4.92$), especially when the plant's nutrient uptake rate was also low ($a_P * r_P \leq 0.02$; Figure 4(b)). Interactions outside of these ranges mostly fell into the stable dynamical regime, with smaller frequencies of the other regimes also possible.

Discussion

Overview

Despite the foundational role they play in plant communities and global nutrient cycling (Smith & Read, 2010; van der Heijden et al., 2015), we lack a comprehensive understanding of the dynamics of plant-mycorrhizal interactions. Such an understanding would not only increase our ability to conserve natural plant-fungal communities facing the combined threats of global change (Staddon et al., 2002; Steidinger et al., 2020; Van Diepen et al., 2007) but also enhance the application of mycorrhizae in agricultural and restoration contexts, which often encounter uncertain outcomes (Corrêa et al., 2012; Solaiman & Mickan, 2014). These uncertainties may

well be due to destabilizing dynamics (such as Allee effects and oscillations) that may well occur in these systems but, due to the below-ground nature of plant-mycorrhizal interactions, are hard to observe or even predict.

Here we take a step toward filling this gap by developing a mechanistic, predictive framework for plant-mycorrhizal interactions. Our aim is to help empiricists working on these interactions to identify key dynamics and their drivers by testing predictions of mathematical models with measurable parameters and state variables. The novelty of our approach is threefold. First, we develop a mechanistic theoretical framework that integrates both the consumptive and facilitative aspects of plant-mycorrhizal interactions. Second, we explicitly consider nutrient-plant dynamics thus connecting below-ground and above-ground processes in a single framework. Third, we parameterize the model with extensive empirical data from the literature, which allows us to make reasonably accurate predictions of the possible dynamics and long-term outcomes of real plant-mycorrhizal interactions.

We report three key findings. First, we find that plant-mycorrhizal interactions can exhibit a wide range of dynamics, including Allee effects as well as persistent consumer-resource oscillations. Second, we find that these dynamics can be inferred using measurable parameters and plant and fungal biomass patterns in the field. Third, we find a strong impact of nutrient availability on plant-mycorrhizal interactions with nutrient scarcity increasing the incidence of Allee effects and deterministic extinction at low abundances and nutrient enrichment inducing consumer-resource oscillations in otherwise stable systems, or amplifying existing oscillations to the point of interaction collapse. Below we discuss how these findings can guide further experimental work as well as the restoration of degraded communities.

Inferring plant-mycorrhizal dynamics

354 The ability to accurately infer the dynamics of plant-mycorrhizal interactions (and their
355 underlying drivers) is essential in restoration. Restoration efforts in which both native plant
356 species and fungal symbionts are introduced at low initial biomasses may fail due to hidden
357 Allee effects that cause extinction when initial biomasses are insufficiently high (Armstrong &
358 Wittmer, 2011; Deredec & Courchamp, 2007). Whether this accounts for the often-unpredictable
359 success of mycorrhizal inoculation is not yet known (but see Verbruggen et al., 2013). Based on
360 our parameter space investigation, Allee effects are likely prevalent in many plant-mycorrhizal
361 associations, especially those in which the fungus is more facilitative than consumptive and those
362 in nutrient-poor habitats. The ability to infer the existence of Allee effects based on measurable
363 parameters and biomass patterns (e.g., a steady decline in plant and fungal biomasses following
364 inoculation) would greatly aid managers engaging in restoration efforts to introduce fungal
365 inoculants in sufficiently high initial biomass and to supplement nutrients if the soils tend to be
366 nutrient-poor.

367 More generally, our mechanistic framework and decision tree analysis provide a
368 quantitative roadmap that empiricists can use to infer the dynamics of the specific plant-
369 mycorrhizal systems being studied. The specific parameter thresholds we identified correspond
370 to a three-branching decision tree, but our available simulation data can be used to generate
371 diagnostic trees of any depth or precision. For a given plant-mycorrhizal system, dynamics can
372 be predicted by measuring key parameters and following the decision key diagnostic protocol. As
373 we have shown, whether or not a given interaction is likely to exhibit an Allee effect can be
374 determined by the plant's nutrient uptake rate in the absence of the fungus ($a_P * r_P$) and the
375 fungus' consumption efficiency at low plant biomass ($\frac{m_{AP}}{H}$) (Figure 4 (b)). While the former can
376 be measured using a number of well-established methods (e.g., Chapin & Van Cleve, 2000; Weih

et al., 2018, and citations therein), the latter requires fitting Monod growth curves for mycorrhizal fungi (Monod, 1949). This can be done by introducing fungal inoculates across a range of available host root biomass and measuring fungal biomass growth rates or a proxy such as hyphal growth, optical density, or root colonization (Hameed et al., 2024; Schnepf et al., 2007, 2016).

The role of nutrient availability in driving plant-mycorrhizal interactions

Our results show the overriding importance of soil nutrient availability in driving the dynamics of plant-mycorrhizal interactions, with important implications for agriculture, restoration, and conservation. Nutrient depletion increases the plant's dependence on the fungus, increasing the likelihood of both Allee effects and interaction collapse due to divergent oscillations; nutrient surplus reduces this dependence but can lead to consumer-resource oscillations reminiscent of the paradox of enrichment (Rosenzweig, 1971). While we only considered moderate (20%) increase or decrease in nutrient availability, natural plant-mycorrhizal communities exposed to increased Nitrogen or Phosphorous deposition from fertilizer runoff or soil degradation via logging and agricultural intensification may experience much higher levels of enrichment and depletion (Dentener et al., 2006; Kopittke et al., 2017; Marx et al., 2019; Murty et al., 2002).

Nutrient supply change in either direction can destabilize plant-mycorrhizal interactions, increasing their extinction risk. A nutrient deficit in the soil can cause fungal biomass to fall below the Allee threshold, causing deterministic extinction of the fungus. In contrast, a nutrient surplus can cause divergent oscillations leading to interaction collapse, especially when the fungus has a high maximum uptake rate (m_{AP}) and a low half-saturation density (H). Even in oscillatory systems not subject to deterministic interaction collapse, the high-amplitude

400 oscillations under enrichment can predispose species to extinction via demographic stochasticity
401 during periods of low biomass densities. Temporal and spatial variation in nutrient availability,
402 commonly observed in many plant communities (Jackson & Caldwell, 1993; Xue et al., 2019),
403 could not only affect where a plant-mycorrhizal interaction can establish, but also how it
404 functions and whether it is prone to extinction due to dynamical instabilities. Our findings
405 highlight the critical role that nutrient supply plays in the context dependency of plant-
406 mycorrhizal interactions, emphasizing the importance of measuring soil nutrient availability
407 prior to inoculating the soil during restoration efforts, or applying additional fertilizer in
408 agricultural settings.

409 In situations where the decision tree protocol is not feasible, our results provide an
410 alternative approach to inferring the dynamics of plant-mycorrhizal interactions. The existence of
411 an Allee effect can be inferred by comparing long-term plant growth without and without a
412 mycorrhizal inoculum across a range of soil nutrient densities. As predicted by our analyses, an
413 Allee effect is likely to be present if the plant's long-term biomass is increased by the presence of
414 a fungal symbiont (Figure 1). Our finding is that there is a critical nutrient supply below which
415 the facilitative component of the fungus' interaction with the plant exceeds the consumptive
416 component causing an increase in the plant's long-term biomass in the presence of the fungus.
417 Above this threshold, the fungus either reduces the long-term plant biomass if the interaction is
418 stable or causes persistent or divergent fluctuations in plant and fungal abundances. It is possible
419 to distinguish between these outcomes by recording plant and fungal biomasses across a range of
420 soil nutrient availability, and comparing biomasses with and without the fungus and determining
421 whether biomasses remain relatively stable over time or exhibit fluctuations. Repeating this
422 process for several commercially available fungal inoculants, crop species, and nutrient

conditions is admittedly time consuming and labor intensive but can yield important insights into choosing inoculants and growing conditions that maximize the efficacy of mycorrhizal applications in restoration and agriculture.

Limitations and future directions

Our model considers a pairwise plant-mycorrhizal interaction that utilizes a single limiting nutrient. This is both because we need to understand the dynamics of pairwise interactions before we consider multi-species communities and for the analytical tractability necessary to generate *a priori* predictions that could be tested via numerical simulations. Extending our model to include multiple-plant fungal interactions utilizing multiple limiting nutrients is an important future direction. Given that plants in most soils are limited primarily by either Nitrogen or Phosphorous (Du et al., 2020; Marx et al., 2019; Menge et al., 2009), incorporating both N and P limitation is a logical next step. Similarly, multiple fungal species may compete for the biomass of shared plant hosts, and both plants and fungi may compete for the mutualistic benefits conferred by partner species (Johnson & Amarasekare, 2013; van der Heijden et al., 2015). Extending our model to incorporate plant and fungal competition can yield broader insights plant-mycorrhizal community persistence in both natural and agricultural settings.

Tables

Table 1: Parameter values and ranges used in the numerical analysis.

Parameter	Value/Range	Units	Citations
Nutrient supply point (**S**)	0.01-7.0[1] (1.0±0.2 used)	g N m^{-2}	Ansong Omari et al., 2018; Pastor et al., 1987
Plant maximum nutrient uptake rate ($\mathbf{a_P}$)	0.17±0.2[2]	g N^{-1} day^{-1}	Marx et al., 2019
Fungus maximum plant C uptake rate ($\mathbf{m_{AP}}$)	0.08-0.17	day^{-1}	Hobbie & Hobbie 2006
Plant half saturation constant (**M**)	0.1-2.0	g	This study
Fungus half saturation constant (**H**)	0.08-36.8	g	This study
Fractional reduction in uptake rate ($\mathbf{r_P}$)	0.0-1.0 (0.0-0.2 used)	None	van der Heijden et al., 2015
Plant Nitrogen:Carbon ratio ($\mathbf{e_P}$)	0.027	g N / g C	Elser et al., 2000, 2010
Fungus Nitrogen:Carbon ratio ($\mathbf{e_A}$)	0.069	g N / g C	Zhang & Elser, 2017
Plant metabolic loss rate ($\mathbf{d_P}$)	0.01	g day^{-1}	Marx et al., 2019
Fungal metabolic loss rate ($\mathbf{d_A}$)	0.03	g day^{-1}	This study

1. Parameter ranges given in this format indicate observed ranges for which there was not an identifiable mean and standard error. For nutrient supply point, we used a median value of 1.0 g N m^{-2} for all simulations.
2. The empirical range for a_{Pi} is given as mean±SE. We used a_{Pi} values in the range 0.07-0.27 g N^{-1} day^{-1} for the simulations, which are within the 95% confidence interval.

Table 2: Occurrence of different plant-mycorrhizal dynamical realms across the empirically observed parameter space. The "All Systems" column indicates the numbers of parameter combinations that were predicted to yield a given dynamical regime based on the asymptotic analyses. The "Persistent Systems" column indicates the same for systems that exhibited long-term persistence in our numerical simulations.

Dynamical Regime	Count	
	All systems (analytical)	Persistent systems (numerical)
Infeasible	80,975	8[1]
No Allee effect, No Oscillations	17,851	17,849
Allee effect, no oscillations	15,437	9,298
Oscillatory, no Allee effect	14,549	5,141
Oscillatory with Allee effect	608	33
Obligate systems[2]	20,580	0
Total	150,000	32,329

[1] All infeasible systems that remained persistent at the end of the simulation run were in a state of transient persistence in which the fungus was decreasing but had not yet crossed the extinction threshold. Increasing simulation runtime by 50% led to extinctions in all 8 cases.

[2] Meaning both the plant *and* fungus are obligate on partners. Such systems are always subject to Allee effects, but we did not differentiate between oscillatory and non-oscillatory, since in our assembly framework all such interactions go extinct before introduction of the fungus.

Figures

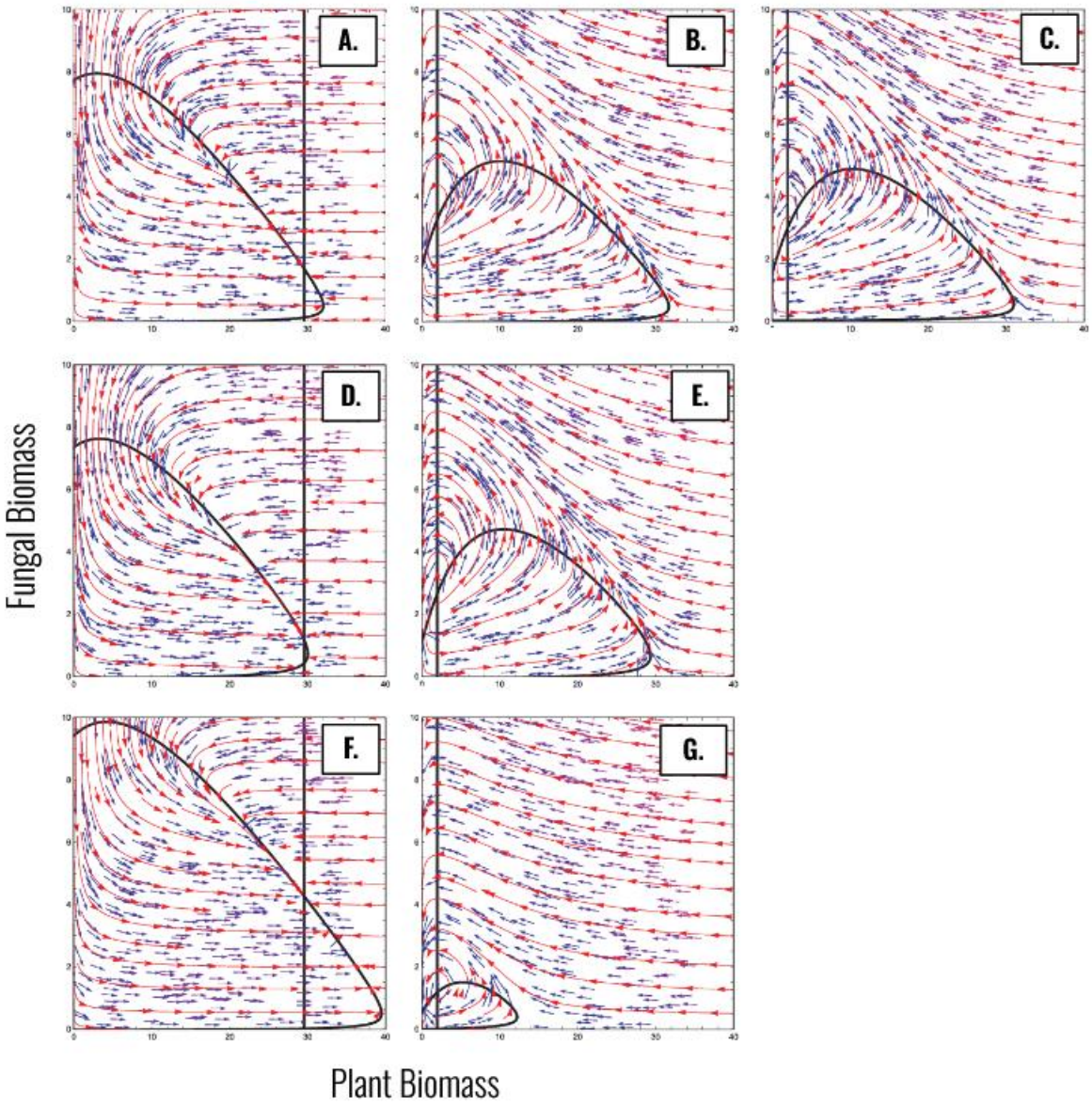

Figure 1: Phase plane diagrams for the plant-mycorrhizal model (Equation (1)). In all panels, the solid black curve and the solid vertical line depict, respectively, the zero growth isoclines for the plant species and the mycorrhizal fungal strain. The points at which the isoclines cross in the interior of the state space constitute interior equilibria with both plant and fungus present; the point at which the plant isocline crosses the x-axis constitutes the boundary equilibrium with only

the plant present. The model yields three dynamical realms (panels (a)-(c)). When the fungal isocline crosses to the right of the maximum of the plant isocline and closer to its vertex (a_P and r_P are low relative to d_P, H is high and m_{AP} is low), the interaction exhibits an Allee effect giving rise to two internal equilibria the larger of which is locally stable and the smaller is locally unstable (panel (a); S=1.0, a_P = 0.2; r_P = 0.1; M = 0.6; m_{AP} = 0.1; H = 9.0; See Appendix 1 for details). When the fungal isocline crosses to the left of the maximum and farther away from the vertex (H is lower and m_{AP} is higher), the Allee effect disappears and there is a single internal equilibrium that is either locally stable or unstable with persistent oscillations around it (panel (b): m_{AP} = 0.15; H = 1.9). As r_P tends to zero and the plant becomes increasingly dependent on the fungus, there is no longer a feasible boundary (plant-only) equilibrium (panel (c); r_P=0.02). Panels (d) and (e) depict the effect of M on the plant-fungal interaction. When there is an Allee effect and M is high (panel (d), M=1.5), the plant's zero growth isocline has a lower maximum and a vertex leading to a lower equilibrium biomass for the fungus (compare panels (a) and (d)). We see the same effect when there is no Allee effect (panel (d), M=1.5; compare panels (b) and (e)). Panels (f) and (g) depict the effect of S on the plant-fungal interaction. When S is relatively high (panel (f), S=1.2), the plant is less dependent on the fungus for nutrient acquisition and the Allee effect disappears (compare panels (a) and (f)). When S is low (panel (g), S=0.8), the plant becomes more dependent on the fungus, making an Allee effect more likely (compare panels (b) and (g)). Parameters common to all panels: e_P=0.027, e_A=0.069, d_P=0.01, d_A=0.03. For panels (b) and (d)-(f), the other parameters same as in panel (a). For panel (c), the other parameters are the same as in panel (b).

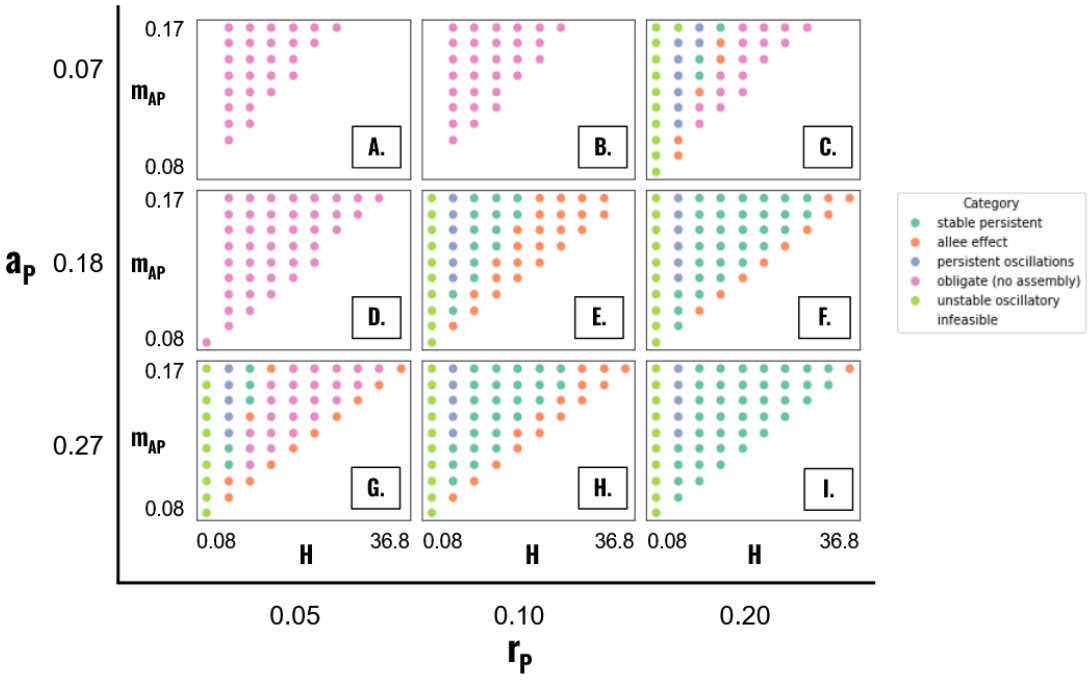

500

501 Figure 2: The effects of key parameters (a_P, r_P, m_{AP}, H) on the dynamical realms exhibited by the plant-
502 mycorrhizal interaction. The main plot depicts the distribution of dynamical regimes as a function
503 of a_P and r_P, while each subplot depicts the distribution as a function of m_{AP}, and H. Because no
504 interactions could assemble when r_P=0, we use the next lowest value (0.05) as the "minimum" for
505 this parameter. The remaining parameters (S, M) are held at their median values. In all subplots, the
506 white regions in the lower right depict the parameter space of infeasible interactions.

507

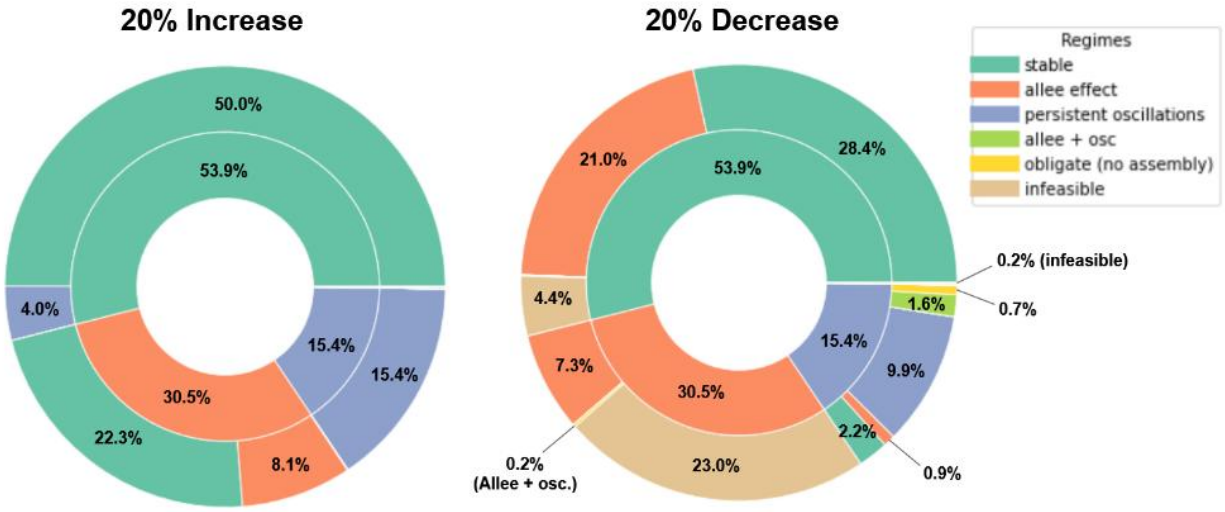

Figure 3: Nested pie charts illustrating the shift in dynamical realms following a change in the soil nutrient supply. In both panels, the inner ring shows the distribution of dynamical realms for persistent plant-mycorrhizal interactions at the baseline nutrient supply point (S = 1.0 g m^{-2}). The outer rings depict the fractional distribution of these regimes after nutrient depletion or enrichment. Both the inner and outer rings add up to 100% (the remainders being made up of trace wedges with annotations omitted here for clarity).

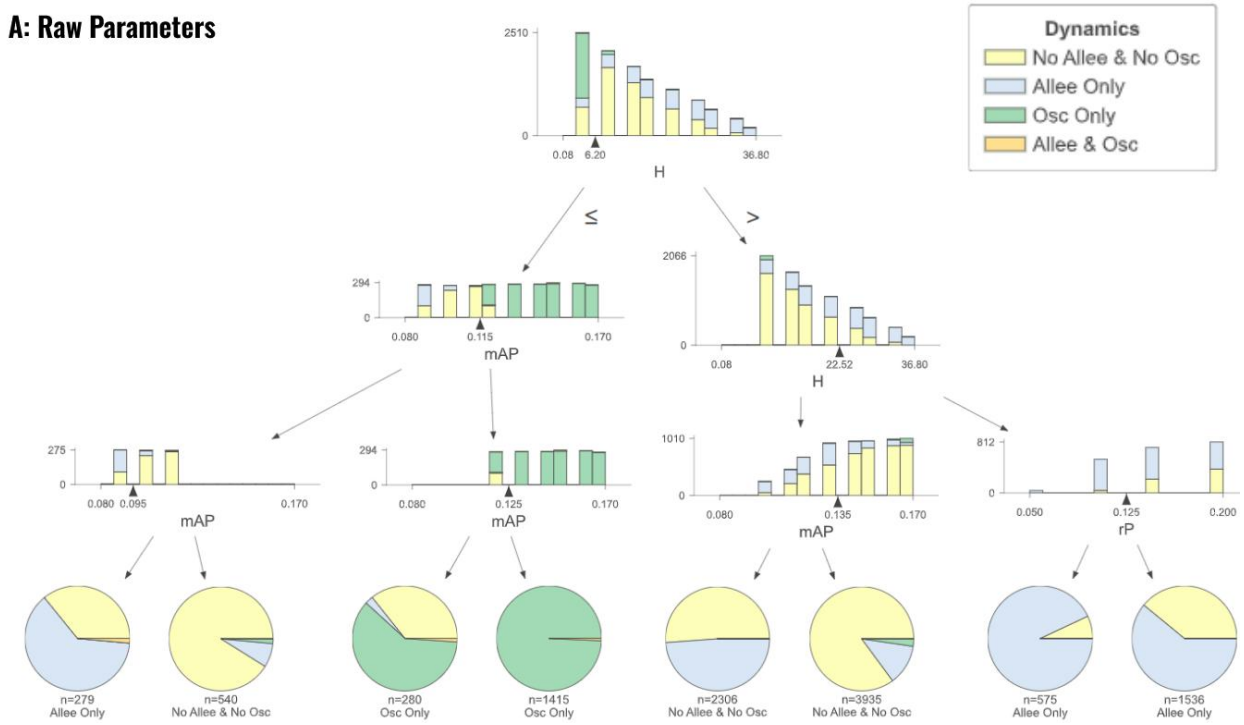

518

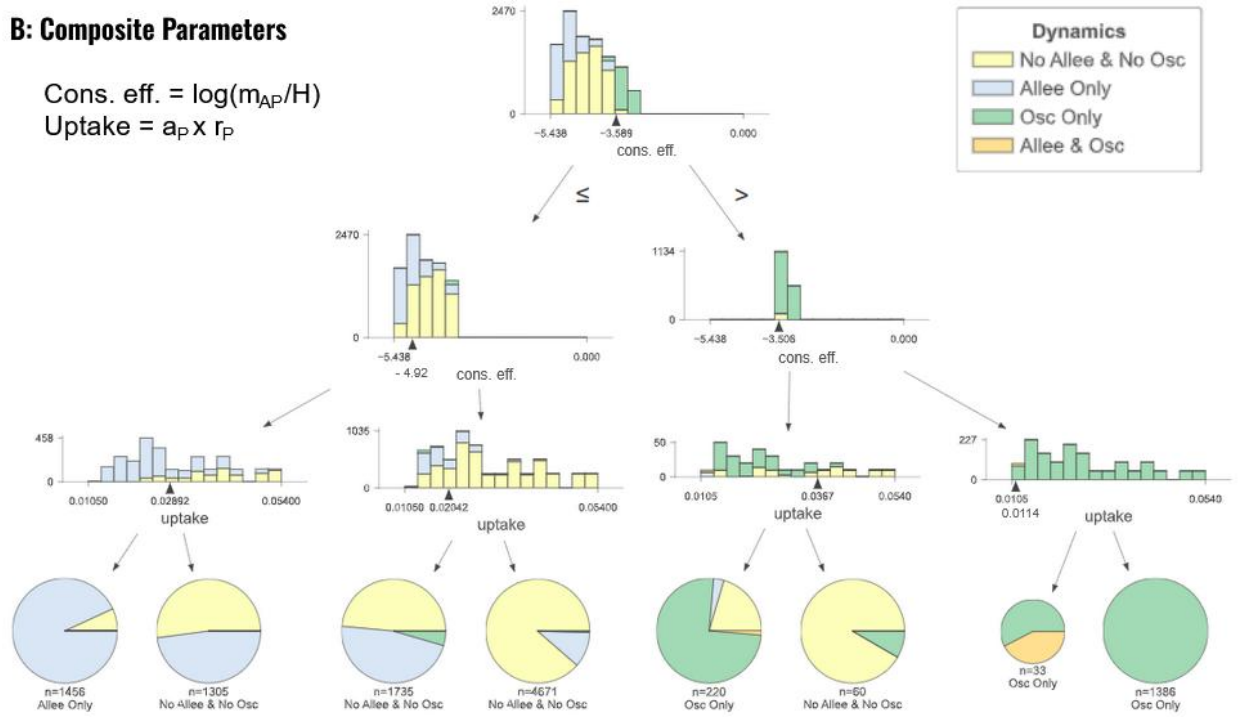

519

520 Figure 4: Decision trees for diagnosing plant-mycorrhizal interaction dynamics based on

521 measurable parameters (A) and combinations thereof (B). Trees were developed based on all

simulated interactions at S=1.0 in which both the plant and fungus were persistent at the end of the simulation run.

Literature Cited

Ågren, G. I., Wetterstedt, J. Å. M., & Billberger, M. F. K. (2012). Nutrient limitation on terrestrial plant growth – modeling the interaction between nitrogen and phosphorus. *New Phytologist*, *194*(4), 953–960. https://doi.org/10.1111/j.1469-8137.2012.04116.x

Aguilar-Trigueros, C. A., Rillig, M. C., & Crowther, T. W. (2017). Applying allometric theory to fungi. *The ISME Journal*, *11*(10), Article 10. https://doi.org/10.1038/ismej.2017.86

Ansong Omari, R., Bellingrath-Kimura, D. S., Fujii, Y., Sarkodee-Addo, E., Appiah Sarpong, K., & Oikawa, Y. (2018). Nitrogen Mineralization and Microbial Biomass Dynamics in Different Tropical Soils Amended with Contrasting Organic Resources. *Soil Systems*, *2*(4), Article 4. https://doi.org/10.3390/soilsystems2040063

Armstrong, D. P., & Wittmer, H. U. (2011). Incorporating Allee effects into reintroduction strategies. *Ecological Research*, *26*(4), 687–695. https://doi.org/10.1007/s11284-011-0849-9

Asmelash, F., Bekele, T., & Birhane, E. (2016). The Potential Role of Arbuscular Mycorrhizal Fungi in the Restoration of Degraded Lands. *Frontiers in Microbiology*, *7*. https://doi.org/10.3389/fmicb.2016.01095

Brundrett, M. C. (2009). Mycorrhizal associations and other means of nutrition of vascular plants: Understanding the global diversity of host plants by resolving conflicting information and developing reliable means of diagnosis. *Plant and Soil*, *320*(1), 37–77. https://doi.org/10.1007/s11104-008-9877-9

Bryant, R. L., & Bever, J. D. (n.d.). Context dependence of grassland plant response to arbuscular mycorrhizal fungi: The influence of plant successional status and soil resources. *Journal of Ecology*, *n/a*(n/a). https://doi.org/10.1111/1365-2745.14424

Chapin, F. S., & Van Cleve, K. (2000). Approaches to studying nutrient uptake, use and loss in plants. In R. W. Pearcy, J. R. Ehleringer, H. A. Mooney, & P. W. Rundel (Eds.), *Plant Physiological Ecology: Field methods and instrumentation* (pp. 185–207). Springer Netherlands. https://doi.org/10.1007/978-94-010-9013-1_10

Corrêa, A., Gurevitch, J., Martins-Loução, M. A., & Cruz, C. (2012). C allocation to the fungus is not a cost to the plant in ectomycorrhizae. *Oikos*, *121*(3), 449–463. https://doi.org/10.1111/j.1600-0706.2011.19406.x

Dentener, F., Drevet, J., Lamarque, J. F., Bey, I., Eickhout, B., Fiore, A. M., Hauglustaine, D., Horowitz, L. W., Krol, M., Kulshrestha, U. C., Lawrence, M., Galy-Lacaux, C., Rast, S., Shindell, D., Stevenson, D., Van Noije, T., Atherton, C., Bell, N., Bergman, D., … Wild, O. (2006). Nitrogen and sulfur deposition on regional and global scales: A multimodel evaluation. *Global Biogeochemical Cycles*, *20*(4). https://doi.org/10.1029/2005GB002672

Deredec, A., & Courchamp, F. (2007). Importance of the Allee effect for reintroductions. *Écoscience*, *14*(4), 440–451. https://doi.org/10.2980/1195-6860(2007)14[440:IOTAEF]2.0.CO;2

Du, E., Terrer, C., Pellegrini, A. F. A., Ahlström, A., van Lissa, C. J., Zhao, X., Xia, N., Wu, X., & Jackson, R. B. (2020). Global patterns of terrestrial nitrogen and phosphorus limitation. *Nature Geoscience*, *13*(3), Article 3. https://doi.org/10.1038/s41561-019-0530-4

Elser, J. J., Fagan, W. F., Denno, R. F., Dobberfuhl, D. R., Folarin, A., Huberty, A., Interlandi, S., Kilham, S. S., McCauley, E., Schulz, K. L., Siemann, E. H., & Sterner, R. W. (2000). Nutritional

constraints in terrestrial and freshwater food webs. *Nature*, *408*(6812), Article 6812. https://doi.org/10.1038/35046058

Elser, J. J., Fagan, W. F., Kerkhoff, A. J., Swenson, N. G., & Enquist, B. J. (2010). Biological stoichiometry of plant production: Metabolism, scaling and ecological response to global change. *New Phytologist*, *186*(3), 593–608. https://doi.org/10.1111/j.1469-8137.2010.03214.x

Fellbaum, C. R., Gachomo, E. W., Beesetty, Y., Choudhari, S., Strahan, G. D., Pfeffer, P. E., Kiers, E. T., & Bücking, H. (2012). Carbon availability triggers fungal nitrogen uptake and transport in arbuscular mycorrhizal symbiosis. *Proceedings of the National Academy of Sciences*, *109*(7), 2666–2671. https://doi.org/10.1073/pnas.1118650109

Fester, T., & Sawers, R. (2011). Progress and Challenges in Agricultural Applications of Arbuscular Mycorrhizal Fungi. *Critical Reviews in Plant Sciences*, *30*(5), 459–470. https://doi.org/10.1080/07352689.2011.605741

Godbold, D. L., Hoosbeek, M. R., Lukac, M., Cotrufo, M. F., Janssens, I. A., Ceulemans, R., Polle, A., Velthorst, E. J., Scarascia-Mugnozza, G., De Angelis, P., Miglietta, F., & Peressotti, A. (2006). Mycorrhizal Hyphal Turnover as a Dominant Process for Carbon Input into Soil Organic Matter. *Plant and Soil*, *281*(1), 15–24. https://doi.org/10.1007/s11104-005-3701-6

Grover, J. P. (1994). Assembly Rules for Communities of Nutrient-Limited Plants and Specialist Herbivores. *The American Naturalist*, *143*(2), 258–282. https://doi.org/10.1086/285603

Hale, K. R. S., & Valdovinos, F. S. (2021). Ecological theory of mutualism: Robust patterns of stability and thresholds in two-species population models. *Ecology and Evolution*, *11*(24), 17651–17671. https://doi.org/10.1002/ece3.8453

589 Hameed, T., Motsi, N., Bignell, E., & Tanaka, R. J. (2024). Inferring fungal growth rates from optical
590 density data. *PLOS Computational Biology*, *20*(5), e1012105.
591 https://doi.org/10.1371/journal.pcbi.1012105
592 Hart, M. M., & Reader, R. J. (2002). Host plant benefit from association with arbuscular mycorrhizal
593 fungi: Variation due to differences in size of mycelium. *Biology and Fertility of Soils*, *36*(5),
594 357–366. https://doi.org/10.1007/s00374-002-0539-4
595 Hobbie, E. A. (2006). Carbon Allocation to Ectomycorrhizal Fungi Correlates with Belowground
596 Allocation in Culture Studies. *Ecology*, *87*(3), 563–569. https://doi.org/10.1890/05-0755
597 Hobbie, J. E., & Hobbie, E. A. (2006). 15n in Symbiotic Fungi and Plants Estimates Nitrogen and
598 Carbon Flux Rates in Arctic Tundra. *Ecology*, *87*(4), 816–822. https://doi.org/10.1890/0012-
599 9658(2006)87[816:NISFAP]2.0.CO;2
600 Hoeksema, J. D., Chaudhary, V. B., Gehring, C. A., Johnson, N. C., Karst, J., Koide, R. T., Pringle, A.,
601 Zabinski, C., Bever, J. D., Moore, J. C., Wilson, G. W. T., Klironomos, J. N., & Umbanhowar, J.
602 (2010). A meta-analysis of context-dependency in plant response to inoculation with
603 mycorrhizal fungi. *Ecology Letters*, *13*(3), 394–407. https://doi.org/10.1111/j.1461-
604 0248.2009.01430.x
605 Holland, J. N., & DeAngelis, D. L. (2010). A consumer–resource approach to the density-dependent
606 population dynamics of mutualism. *Ecology*, *91*(5), 1286–1295. https://doi.org/10.1890/09-
607 1163.1
608 Jackson, R. B., & Caldwell, M. M. (1993). The Scale of Nutrient Heterogeneity Around Individual
609 Plants and Its Quantification with Geostatistics. *Ecology*, *74*(2), 612–614.
610 https://doi.org/10.2307/1939320

Johnson, C. A., & Amarasekare, P. (2013). Competition for benefits can promote the persistence of mutualistic interactions. *Journal of Theoretical Biology*, *328*, 54–64. https://doi.org/10.1016/j.jtbi.2013.03.016

Koorem, K., Tulva, I., Davison, J., Jairus, T., Öpik, M., Vasar, M., Zobel, M., & Moora, M. (2017). Arbuscular mycorrhizal fungal communities in forest plant roots are simultaneously shaped by host characteristics and canopy-mediated light availability. *Plant and Soil*, *410*(1), 259–271. https://doi.org/10.1007/s11104-016-3004-0

Kopittke, P. M., Dalal, R. C., Finn, D., & Menzies, N. W. (2017). Global changes in soil stocks of carbon, nitrogen, phosphorus, and sulphur as influenced by long-term agricultural production. *Global Change Biology*, *23*(6), 2509–2519. https://doi.org/10.1111/gcb.13513

Koziol, L., Lubin, T., & Bever, J. D. (2024). An assessment of twenty-three mycorrhizal inoculants reveals limited viability of AM fungi, pathogen contamination, and negative microbial effect on crop growth for commercial products. *Applied Soil Ecology*, *202*, 105559. https://doi.org/10.1016/j.apsoil.2024.105559

Loreau, M. (1994). Material Cycling and the Stability of Ecosystems. *The American Naturalist*, *143*(3), 508–513. https://doi.org/10.1086/285616

Loreau, M. (1995). Consumers as Maximizers of Matter and Energy Flow in Ecosystems. *The American Naturalist*, *145*(1), 22–42. https://doi.org/10.1086/285726

Maltz, M. R., & Treseder, K. K. (2015). Sources of inocula influence mycorrhizal colonization of plants in restoration projects: A meta-analysis. *Restoration Ecology*, *23*(5), 625–634. https://doi.org/10.1111/rec.12231

Marx, J. M., Rall, B. C., Phillips, H. R. P., & Brose, U. (2019). Opening the black box of plant nutrient uptake under warming predicts global patterns in community biomass and biological carbon storage. *Oikos*, *128*(10), 1503–1514. https://doi.org/10.1111/oik.06141

McGEE, P. A., Pattinson, G. S., Heath, R. A., Newman, C. A., & Allen, S. J. (1997). Survival of propagules of arbuscular mycorrhizal fungi in soils in eastern Australia used to grow cotton. *The New Phytologist*, *135*(4), 773–780. https://doi.org/10.1046/j.1469-8137.1997.00709.x

Menge, D. N. L., Pacala, S. W., & Hedin, L. O. (2009). Emergence and Maintenance of Nutrient Limitation over Multiple Timescales in Terrestrial Ecosystems. *The American Naturalist*, *173*(2), 164–175. https://doi.org/10.1086/595749

Monod, J. (1949). The Growth of Bacterial Cultures. *Annual Review of Microbiology*, *3*(1), 371–394. https://doi.org/10.1146/annurev.mi.03.100149.002103

Murty, D., Kirschbaum, M. U. F., Mcmurtrie, R. E., & Mcgilvray, H. (2002). Does conversion of forest to agricultural land change soil carbon and nitrogen? A review of the literature. *Global Change Biology*, *8*(2), 105–123. https://doi.org/10.1046/j.1354-1013.2001.00459.x

Nara, K. (2006a). Ectomycorrhizal networks and seedling establishment during early primary succession. *New Phytologist*, *169*(1), 169–178. https://doi.org/10.1111/j.1469-8137.2005.01545.x

Nara, K. (2006b). Pioneer dwarf willow may facilitate tree succession by providing late colonizers with compatible ectomycorrhizal fungi in a primary successional volcanic desert. *New Phytologist*, *171*(1), 187–198. https://doi.org/10.1111/j.1469-8137.2006.01744.x

Neuenkamp, L., Prober, S. M., Price, J. N., Zobel, M., & Standish, R. J. (2019). Benefits of mycorrhizal inoculation to ecological restoration depend on plant functional type, restoration context and time. *Fungal Ecology*, *40*, 140–149. https://doi.org/10.1016/j.funeco.2018.05.004

Neuhauser, C., & Fargione, J. E. (2004). A mutualism–parasitism continuum model and its application to plant–mycorrhizae interactions. *Ecological Modelling*, *177*(3), 337–352. https://doi.org/10.1016/j.ecolmodel.2004.02.010

Pastor, J., Stillwell, M. A., & Tilman, D. (1987). Nitrogen mineralization and nitrification in four Minnesota old fields. *Oecologia*, *71*(4), 481–485. https://doi.org/10.1007/BF00379285

Pepe, A., Giovannetti, M., & Sbrana, C. (2018). Lifespan and functionality of mycorrhizal fungal mycelium are uncoupled from host plant lifespan. *Scientific Reports*, *8*(1), Article 1. https://doi.org/10.1038/s41598-018-28354-5

Rosenzweig, M. L. (1971). Paradox of Enrichment: Destabilization of Exploitation Ecosystems in Ecological Time. *Science*, *171*(3969), 385–387. https://doi.org/10.1126/science.171.3969.385

Ryan, M. H., & Graham, J. H. (2002). Is there a role for arbuscular mycorrhizal fungi in production agriculture? In S. E. Smith & F. A. Smith (Eds.), *Diversity and Integration in Mycorrhizas* (pp. 263–271). Springer Netherlands. https://doi.org/10.1007/978-94-017-1284-2_26

Sapsford, S. J., Paap, T., Hardy, G. E. St. J., & Burgess, T. I. (2017). The 'chicken or the egg': Which comes first, forest tree decline or loss of mycorrhizae? *Plant Ecology*, *218*(9), 1093–1106. https://doi.org/10.1007/s11258-017-0754-6

Schnepf, A., Leitner, D., Schweiger, P. F., Scholl, P., & Jansa, J. (2016). L-System model for the growth of arbuscular mycorrhizal fungi, both within and outside of their host roots. *Journal of The Royal Society Interface*, *13*(117), 20160129. https://doi.org/10.1098/rsif.2016.0129

Schnepf, A., Roose, T., & Schweiger, P. (2007). Growth model for arbuscular mycorrhizal fungi. *Journal of The Royal Society Interface*, *5*(24), 773–784. https://doi.org/10.1098/rsif.2007.1250

Schubert, A., Marzachí, C., MazziTelli, M., Cravero, M. C., & Bonfante-Fasolo, P. (1987). Development of Total and Viable Extraradical Mycelium in the Vesicular–Arbuscular Mycorrhizal Fungus Glomus Clarum Nicol. & Schenck. *New Phytologist*, *107*(1), 183–190. https://doi.org/10.1111/j.1469-8137.1987.tb04892.x

682 Smith, S. E., & Read, D. J. (2010). *Mycorrhizal Symbiosis*. Academic Press.

683 Solaiman, Z. M., & Mickan, B. (2014). Use of Mycorrhiza in Sustainable Agriculture and Land
684 Restoration. In Z. M. Solaiman, L. K. Abbott, & A. Varma (Eds.), *Mycorrhizal Fungi: Use in*
685 *Sustainable Agriculture and Land Restoration* (pp. 1–15). Springer.
686 https://doi.org/10.1007/978-3-662-45370-4_1

687 Staddon, P. L., Heinemeyer, A., & Fitter, A. H. (2002). Mycorrhizas and global environmental change:
688 Research at different scales. *Plant and Soil*, *244*(1), 253–261.
689 https://doi.org/10.1023/A:1020285309675

690 Staddon, P. L., Ramsey, C. B., Ostle, N., Ineson, P., & Fitter, A. H. (2003). Rapid Turnover of Hyphae
691 of Mycorrhizal Fungi Determined by AMS Microanalysis of 14C. *Science*, *300*(5622), 1138–
692 1140. https://doi.org/10.1126/science.1084269

693 Steidinger, B. S., Bhatnagar, J. M., Vilgalys, R., Taylor, J. W., Qin, C., Zhu, K., Bruns, T. D., & Peay, K. G.
694 (2020). Ectomycorrhizal fungal diversity predicted to substantially decline due to climate
695 changes in North American Pinaceae forests. *Journal of Biogeography*, *47*(3), 772–782.
696 https://doi.org/10.1111/jbi.13802

697 Stephens, P. A., Sutherland, W. J., & Freckleton, R. P. (1999). What Is the Allee Effect? *Oikos*, *87*(1),
698 185–190. https://doi.org/10.2307/3547011

699 Tilman, D. (1986). Nitrogen-Limited Growth in Plants from Different Successional Stages. *Ecology*,
700 *67*(2), 555–563. https://doi.org/10.2307/1938598

701 van der Heijden, M. G. A., Martin, F. M., Selosse, M.-A., & Sanders, I. R. (2015). Mycorrhizal ecology
702 and evolution: The past, the present, and the future. *New Phytologist*, *205*(4), 1406–1423.
703 https://doi.org/10.1111/nph.13288

Van Diepen, L. T. A., Lilleskov, E. A., Pregitzer, K. S., & Miller, R. M. (2007). Decline of arbuscular mycorrhizal fungi in northern hardwood forests exposed to chronic nitrogen additions. *New Phytologist*, *176*(1), 175–183. https://doi.org/10.1111/j.1469-8137.2007.02150.x

Verbruggen, E., van der Heijden, M. G. A., Rillig, M. C., & Kiers, E. T. (2013). Mycorrhizal fungal establishment in agricultural soils: Factors determining inoculation success. *New Phytologist*, *197*(4), 1104–1109. https://doi.org/10.1111/j.1469-8137.2012.04348.x

Vitousek, P. M., Hedin, L. O., Matson, P. A., Fownes, J. H., & Neff, J. (1998). Within-System Element Cycles, Input-Output Budgets, and Nutrient Limitation. In M. L. Pace & P. M. Groffman (Eds.), *Successes, Limitations, and Frontiers in Ecosystem Science* (pp. 432–451). Springer. https://doi.org/10.1007/978-1-4612-1724-4_18

Vogelsang, K. M., & Bever, J. D. (2009). Mycorrhizal densities decline in association with nonnative plants and contribute to plant invasion. *Ecology*, *90*(2), 399–407. https://doi.org/10.1890/07-2144.1

Wang, B., & Qiu, Y.-L. (2006). Phylogenetic distribution and evolution of mycorrhizas in land plants. *Mycorrhiza*, *16*(5), 299–363. https://doi.org/10.1007/s00572-005-0033-6

Weih, M., Hamnér, K., & Pourazari, F. (2018). Analyzing plant nutrient uptake and utilization efficiencies: Comparison between crops and approaches. *Plant and Soil*, *430*(1), 7–21. https://doi.org/10.1007/s11104-018-3738-y

Xue, W., Bezemer, T. M., & Berendse, F. (2019). Soil heterogeneity and plant species diversity in experimental grassland communities: Contrasting effects of soil nutrients and pH at different spatial scales. *Plant and Soil*, *442*(1), 497–509. https://doi.org/10.1007/s11104-019-04208-5

Zhang, J., & Elser, J. J. (2017). Carbon:Nitrogen:Phosphorus Stoichiometry in Fungi: A Meta-Analysis. *Frontiers in Microbiology*, *8*, 1281. https://doi.org/10.3389/fmicb.2017.01281

Statements and Declarations

Funding

This work was supported by an NIH Systems and Integrative Biology Training Grant to TD.

Competing Interests

The authors have no relevant financial or non-financial interests to disclose.

Appendix 1: Asymptotic analyses of the plant-mycorrhizal model

Equation (1) admits four equilibria: the trivial equilibrium $\{P^*, A^*\} = \{0, 0\}$, the boundary equilibrium $P_0^* = \frac{a_P r_P S - d_P}{e_P a_P r_P}, S > \frac{d_P}{a_P r_P}, A^* = 0$, and two interior equilibria:

$$P_A^* = \frac{e_A d_A H}{e_P m_{AP} - e_A d_A}, e_P m_{AP} > e_A d_A, \qquad A_{1,2}^* = \frac{-\beta \pm \sqrt{\beta^2 - 4\alpha\gamma}}{2\alpha},$$

in which

$$\alpha = -e_A a_P - e_A a_P r_P - \left(\frac{m_{AP}}{P_A^* + H}\right)$$

$$\beta = a_P(S - e_P P_A^*)(1 + r_P) - e_A a_P r_P M - \left(\frac{m_{AP} M}{P_A^* + H}\right) - d_P$$

$$\gamma = a_P r_P M(S - e_P P_A^*) - d_P M$$

The Jacobian matrix for Equation (1) yields the following elements:

$$f_{PP} = \frac{\partial \frac{dP}{dt}}{\partial P} = \left(\frac{m_{AP}}{H + P^*}\right)^2 A^* P^* - \frac{m_{AP}}{H + P^*} A^* + a_P \left(\frac{A^*}{A^* + M} + r_P\right)(N - e_P P^*) - d_P$$

$$f_{PA} = \frac{\partial \frac{dP}{dt}}{\partial A} = -a_P e_A \left(\frac{A^*}{A^* + M} + r_P\right) P^* + a_P \frac{MNP^*}{(A^* + M)^2} - \frac{m_{AP} P^*}{H + P^*}$$

$$f_{AP} = \frac{\partial \frac{dA}{dt}}{\partial P} = \frac{e_P m_{AP} H A^*}{e_A (H + P^*)^2}$$

$$f_{AA} = \frac{\partial \frac{dA}{dt}}{\partial A} = \frac{e_P m_{AP} P^*}{e_A (H + P^*)} - d_A$$

where $N = S - e_P P^* - e_A A^*$, with P^*, A^* denoting the equilibrium biomasses of the plant and fungus. The Trace and Determinant of the Jacobian matrix are, respectively:

$$Tr(\boldsymbol{J}) = f_{PP} + f_{AA}$$

$$Det(\boldsymbol{J}) = f_{PP} * f_{AA} - f_{PA} * f_{AP}$$

A given equilibrium is stable to small perturbations in its vicinity if $Tr(\boldsymbol{J}) < 0$ and $Det(\boldsymbol{J}) > 0$. The plant experiences strict nutrient limitation, which means that $N \to 0$, i.e., in the presence of the mutualist, nearly all of the available nutrient is taken up by the plant. This in turn means that $f_{PP} < 0$. The fungus does not experience any self-limitation which means that $f_{AA} = 0$, which we can verify by evaluating it at the interior equilibrium $P^* = \frac{e_A d_A H}{e_P m_{AP} - e_A d_A}$. This means that $Tr(\boldsymbol{J}) = f_{PP}$ and $Det(\boldsymbol{J}) = -f_{PA} * f_{AP}$. We see by inspection that $f_{AP} > 0$ as long as $\{P^*, A^*\} > \{0,0\}$. That leaves us with the sign of f_{PA}. Since $N \to 0, \frac{a_P MN}{M + A^*} \to 0$ and $f_{PA} < 0$ as long as the plant is nutrient-limited.

The key point to appreciate is that while Equation (1) differs from a standard consumer-resource model in that the consumer (fungus) provides a benefit to the resource (plant), it retains the fundamentally antagonistic nature of a consumer-resource interaction with the off-diagonal Jacobian elements exhibiting opposite signs ($f_{PA} < 0,\ f_{AP} > 0$). However, the fact that the fungus aids the plant in acquiring nutrients while removing carbohydrates leads to the emergence of an Allee effect, thus fundamentally altering the dynamics of the interaction such that unlike in

766 a standard consumer-resource model, there are multiple stable equilibria and the long-term
767 outcomes depend on initial condition (see main text for details). In the following sections we
768 present the stability analyses for each of the four fixed points. Henceforth, we refer to the plant
769 biomass at the boundary fixed point as P_0^* and at the interior fixed point(s) as P_A^*.

770 *Local Stability of the trivial equilibrium*

771 Evaluated at $\{P^*, A^*\} = \{0,0\}$, all elements of the Jacobian matrix are ≤ 0 except
772 $f_{PP}(0,0) = Sa_P r_P - d_P$, which is the condition for a facultative plant. If $Sa_P r_P > d_P$, then
773 $Det(\boldsymbol{J}) < 0$; the fixed point is unstable and the plant will increase from a small initial abundance
774 until it reaches the boundary equilibrium $(P_0^*, 0)$. If $Sa_P r_P < d_P$, all eigenvalues of the Jacobian
775 are negative and the trivial equilibrium is locally stable.

776 *Local Stability of the boundary equilibrium*

777 When the plant is facultative ($r_P > 0$), the Jacobian elements evaluated at the boundary
778 equilibrium are:

779 $$f_{PP}(P_0^*, 0) = d_P - Sa_P r_P,$$

780 $$f_{PA}(P_0^*, 0) = (Sa_P r_P - d_P)\left(-\frac{e_A}{e_P} - \frac{m_{AP}}{(Ha_P e_P r_P + Sa_P r_P - d_P)} + \frac{d_P}{Me_P a_P r_P^2}\right),$$

781 $$f_{AP}(P_0^*, 0) = 0$$

782 $$f_{AA}(P_0^*, 0) = -d_A + \frac{m_{AP}(Sa_P r_P - d_P)}{a_P e_A r_P\left(H + \frac{Sa_P r_P - d_P}{a_P e_P r_P}\right)}.$$

783 In examining the Jacobian elements $f_{PP}(P_0^*, 0)$ is always negative since $r_P > 0$;
784 $f_{PA}(P_0^*, 0)$ is positive if $P_0^* > \frac{m_{AP}}{\left(\frac{d_P}{r_P M}\right) - a_P r_P e_A} - H$. This inequality is always satisfied for a

785 facultative plant species within the empirical parameter space we investigated.

786 $f_{AP}(P_0^*, 0) = 0$ always and $f_{AA}(P_0^*, 0) > 0$ if $\frac{d_A e_A H}{m_{AP} e_P - d_A e_A} < \frac{S a_P r_P - d_P}{e_P a_P r_P}$ where $\frac{d_A e_A H}{m_{AP} e_P - d_A e_A}$ is the

787 equilibrium plant biomass in the presence of the fungus (P_A^*) and $\frac{S a_P r_P - d_P}{e_P a_P r_P}$ is the equilibrium

788 plant biomass in the absence of the fungus (P_0^*). If $f_{AA}(P_0^*, 0) > 0$ *and* $|f_{AA}(P_0^*, 0)| >$

789 $|f_{PP}(P_0^*, 0)|$, then $Tr(\boldsymbol{J}) > 0$, $Det(\boldsymbol{J}) < 0$, and the boundary equilibrium is unstable, i.e., an

790 initial introduction of fungus will cause the system to move away from the $(P_0^*, 0)$. If the above

791 condition is not met, the boundary equilibrium will be locally stable and attract nearby initial

792 conditions.

793 *Local stability of the lower interior equilibrium ("Allee threshold")*

794 When $P_0^* < P_A^*$, the fungal nullcline crosses the plant nullcline twice in positive phase

795 space. The complicated nature of the solutions for $A_{1,2}^*$ makes the Jacobian elements evaluated at

796 the lower fixed point (P_A^*, A_1^*) analytically intractable for all but $f_{AA}(P_A^*, A_{1,2}^*)$, which simplifies to

797 zero for both interior fixed points. For the rest, qualitative inferences can be made by analyzing

798 the phase planes and vector fields (Fig. S1).

799 In looking at the phase diagram (Figure S1), $\frac{dA(t)}{dt} < 0$ to the left of the fungal nullcline

800 (P_A^*), and $\frac{dA(t)}{dt} > 0$ to the right of the fungal nullcline. As such, it is apparent that $\frac{\partial \dot{A}}{\partial P} > 0$ for any

801 point on the fungal nullcline, including both (P_A^*, A_1^*) and (P_A^*, A_2^*).

802 Outside the plant nullcline's enclosed ellipsoid, $\frac{dP(t)}{dt} < 0$, while inside $\frac{dP(t)}{dt} > 0$. At the

803 lower fixed point (P_A^*, A_1^*), increasing A brings the populations into the enclosed space, while

804 decreasing A brings them outside of it. Thus, that $f_{PA}(P_A^*, A_1^*) > 0$. Similarly, as the lower

805 equilibrium sits on the undercut of the ellipse (necessarily – if there were no undercut there could

806 not be two positive interior fixed points), increasing P causes $\frac{dP(t)}{dt} < 0$ and *vice versa*. Thus,

807 $f_{PP}(P_A^*, A_1^*) < 0$.

808 Therefore, $Tr(\boldsymbol{J}) < 0$ and $Det(\boldsymbol{J}) < 0$, meaning the lower interior fixed point is locally
809 unstable. The vector fields indicate the point is a saddle approached via trajectories starting to the
810 upper-left and lower-right, and departed via trajectories toward the lower-left (toward the
811 boundary equilibrium) and upper-right (toward the upper interior fixed point). Starting from
812 $(P_0^*, 0)$, an initial biomass of introduced fungus must be great enough so the population trajectory
813 passes through or above this point in order to potentially reach the basin of attraction of the
814 upper interior point – this is the Allee threshold with respect to A(t).

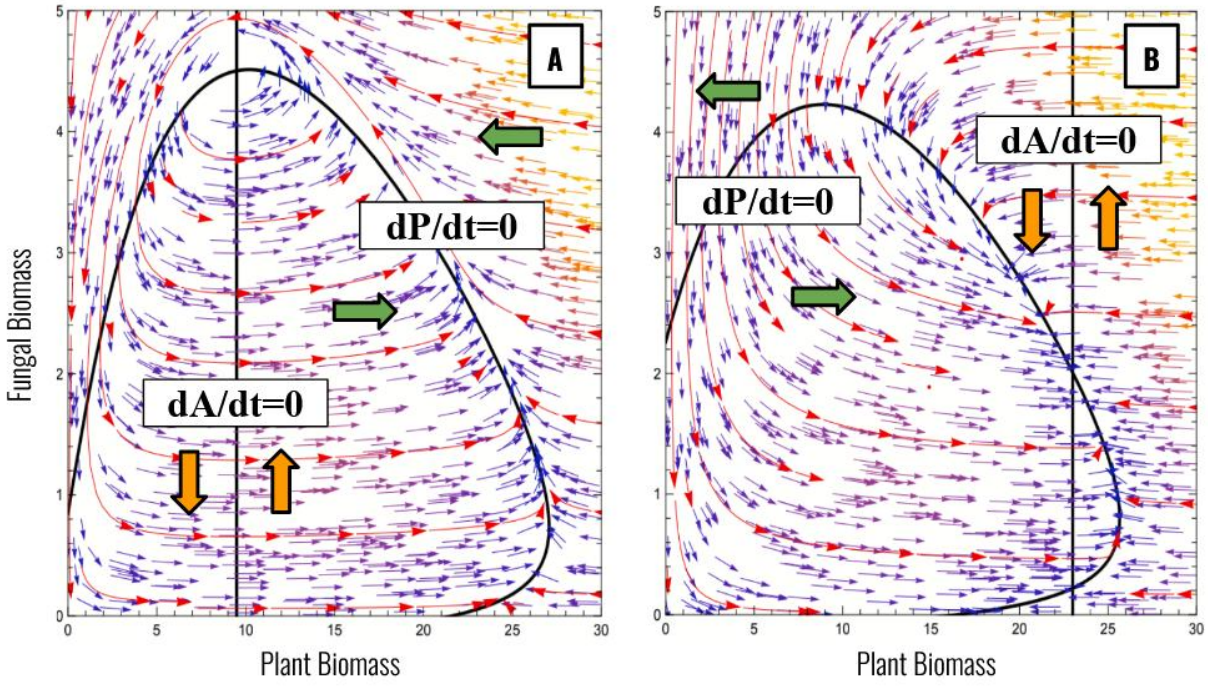

815

816 Figure S1: Annotated phase planes for feasible plant-mycorrhizal interactions. Panel A depicts a
817 system for which $P_A^* < P_0^*$, yielding only one positive interior fixed point (e.g., the lower fixed
818 point has passed into the negative fungal biomass quadrant). Panel B depicts a system for which

819 $P_A^* > P_0^*$, yielding two positive interior fixed points, the lower of which is the Allee threshold.
820 Large green arrows depict population trajectories for along the plant biomass axis within regions
821 delineated by the plant nullcline; orange arrows depict the same for fungal biomass.

822 *Local stability of the upper interior equilibrium*

823 As with the lower interior fixed point, the upper interior fixed point does not lend to
824 tractable analytical expressions for all the Jacobian elements. Once again, $f_{AA}(P_A^*, A_2^*) = 0$ and
825 the rest can be deduced graphically. From the phase plane analysis it is clear that $f_{AP}(P_A^*, A_2^*) > 0$
826 and $f_{PA}(P_A^*, A_2^*) < 0$. However, the sign of $f_{PP}(P_A^*, A_2^*)$ depends on the shape of the plant
827 nullcline and the location of its intersection with the fungal nullcline. In Fig S1B, the position of
828 the upper interior fixed point is such that $f_{PP}(P_A^*, A_2^*) < 0$, giving $Tr(\boldsymbol{J}) < 0$ and $Det(\boldsymbol{J}) > 0$.
829 In this case the upper interior equilibrium is locally stable.

830 If the fungal nullcline crosses to the left of the maximum of the plant nullcline (as in Fig
831 S1A), $f_{PP}(P_A^*, A_2^*) > 0$, giving $Tr(\boldsymbol{J}) > 0$ and $Det(\boldsymbol{J}) > 0$. In this case the upper interior
832 equilibrium is locally unstable and leads to consumer-resource oscillations. Whether these
833 oscillations exist as stable limit cycles around the equilibrium or become divergent, causing the
834 system to collapse to the boundary or trivial equilibria, can only be determined numerically.

835
836